A Comparison of Various Images Processing Methods Used in Evaluation of Liquid Film Disruption

Lucie Měšťanová[1,*] and *Ondřej* Bartoš[1]

[1]CTU in Prague, Energy Engineering Department, Technická 4, Prague 6, 166 07, Czechia

Abstract. The aim of the paper is to introduce and compare various methods which can be used for an image processing. Studied methods include the image pre-processing and the image segmentation based on the Gaussian mixture model and the active contour. The images are acquired within the measurement of the liquid film disruption on the aerofoil's trailing placed edge in the wind tunnel. As the result is suggested sequence of the particular image processing techniques for an optimal result. This work is the part of the wider project devoted to the coarse water droplets which have a negative effect on the steam turbines efficiency and reliability.

1 Introduction

In the long term the Energy engineering department at CTU is concerned with experimental research in the liquid phase structure in steam turbines [1, 2]. In steam turbines, there are presented two groups of water droplets.

The nucleation of droplets and their subsequent growth due to the surface condensation is responsible for the presence of fine droplets. Their expected diameters range is between 200 nm and 800 nm. Coarse droplets are formed by the disruption of water films on the blades and casing surfaces in the low-pressure turbine stages. Their diameters range is very wide, from a few micrometres to one millimetre. They have the negative effect on the reliability and the efficiency of the steam turbines and they are also responsible for unfavourable effects like the additional energy losses or reduction of the blades lifetime. The present knowledge about the coarse water droplets formation, their flow field and the size droplets distribution in turbines is still insufficient. A better understanding of the coarse droplets formation and their properties may provide future enhancements for the steam turbine and other similar applications. Previous measurement of coarse droplets directly in the steam turbine made it necessary to build an experimental tunnel for the study of the droplets formation and their properties [3, 4] in the laboratory.

2 Testing facility

Due to difficulties connected with making measurements in an operating steam turbine, a wind tunnel was designed and manufactured for the analysis of the coarse droplets formation from the liquid films. The goal of the design was to achieve the conditions in the steam turbine as closely as possible together with the advantages of working in the laboratory.

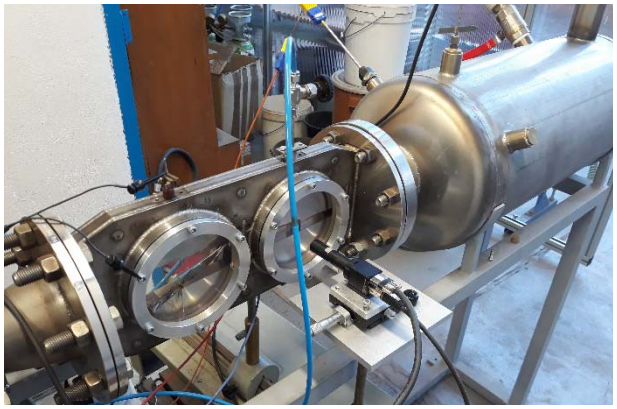

Fig. 1. Wind tunnel test section with camera.

The tunnel is designed as a classical CD nozzle, but the typical operational regime is subsonic or transonic (Fig. 1). The aerofoil, placed in the nozzle, simulates the blade in the turbine and it is possible to remove or replace it. On the aerofoil is a groove for supplying liquid on its surface. The liquid is pumped to the aerofoil surface through the dosing pump with a flow from 1 ml/min to 500 ml/min. The tunnel is equipped with four large optical windows to have a good optical access for the measurements. It is possible to operate the tunnel with the steam in continuous mode or with the compressed air in periodic mode.

Measurement methods

The time of the measurement with the air in the wind tunnel depends on the pressure in the compressor storage vessel. The pressure and temperature of entire

* Corresponding author: lucie.mestanova@fs.cvut.cz

measurement sequence is acquired by the NI SCXI data acquisition system for the flow conditions description. Two methods of droplets size measurement are available. The light scattering method is used for small particles and the photogrammetry is used for bigger droplets and for droplets formation on the aerofoil's trailing edge. The measurement schema is shown in Fig. 2.

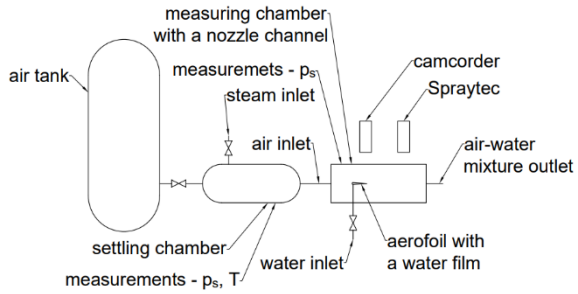

Fig. 2. Measurement schema of the wind tunnel.

The used camera XIMEA MC050CG-SY contains color CMOS digital image sensor Sony IMX250 LQR-C. The sensor has 2464x2056 active pixels and 3,45 µm pixel pitch.

Calibration is required for correct pixel/dimension ratio. The ratio was determined as 1,7 µm/px with help of the calibration target. The light source with variable length of the flash at the order of 0,5-17µs was used.

On the figures below one can see efficiency of the camera chipset and profile of the emitted light from LED.

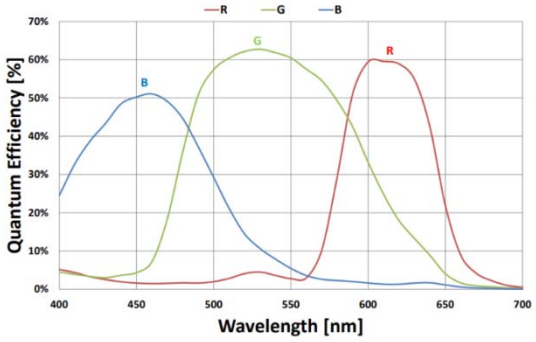

,

Fig. 3. Quantum efficiency of the camera sensor.

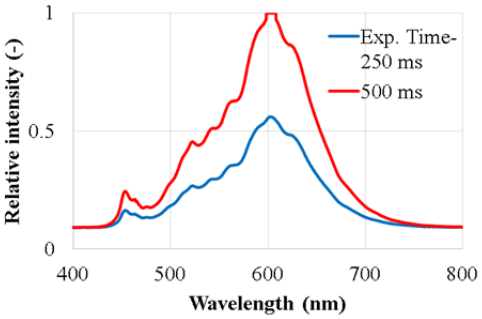

Fig. 4. Characteristic of the used diode with different time of the spectrometer.

The characteristic of the LED light source together with the quantum efficiency of the camera chipset and with involving the light scattering [5] of the light on the liquid leads to the expectation that the best visibility of the liquid film is for green or red channel of the captured image.

3 Image processing methods

The camera captures the images with the size of 3,5x4 mm in the vicinity of the aerofoil. These images are further processed in Matlab. The aim is to evaluate the amount of the water on the image for the description of the disruption process and evaluation of the droplets size distribution. Three segmentation methods were used for this purpose. Enhancement of the histogram was used for the image pre-processing.

3.1. Pre-processing (+entropy)

Enhancement of histogram by linear intensity stretching was used for image pre-processing. Entropy of the image and its parts was determined for the evaluation of the image processing methods. Entropy is a measure of randomness of the image and it is defined as:

$$H_e = -\sum_i p_i \cdot \log_2 p_i \ \text{(bit)} \qquad (1)$$

where p_i is a probability of intensities.

Entropy characterizes the texture of the image. As lower the entropy value is as less noisy is the image. This property is suggested as a value for the compares of the methods

3.2. Thresholding

Thresholding is the simplest segmentation method based on the classification of pixel intensity values. It is necessary to select the most accurate threshold value from the image histogram. Then, pixels with a value below the threshold are classified as the first segment and vice versa.

$$g(x,y) = \begin{cases} 0 & \text{for } f(x,y) \le T \\ 1 & \text{for } f(x,y) > T \end{cases} \qquad (2)$$

where $g(x,y)$ denotes segmented image and $f(x,y)$ its histogram.

3.3. Active contour

Active contour is sophisticated segmentation method also known as the snake method. The input to this method is a closed curve that surrounds the object to be segmented. The curve is evolving, it moves toward its interior and it stops at the object boundary.

The snake model [7] is: $\inf_C J_1(C)$, where

$$J_1(C) = \alpha \int_0^1 |C'(s)|^2 ds + \beta \int_0^1 |C''(s)|^2 ds - \lambda \int_0^1 \left|\nabla u_0(C(s))\right|^2 ds \qquad (3)$$

α, β and λ are positive parameters. The first two conditions control the smoothness of the contour and the third condition push the contour toward the object in the image. The stopping term is based on Mumford-Shah segmentation techniques.

Level set formulation: $C \subset \Omega$ is represented by the zero level set of a Lipschitz function $\phi: \Omega \to \mathbb{R}$, such that

$$\begin{cases} C = \partial\omega = \{(x,y) \in \Omega: \phi(x,y) = 0\} \\ inside(C) = \omega = \{(x,y) \in \Omega: \phi(x,y) > 0\} \\ outside(C) = \Omega \setminus \varpi = \{(x,y) \in \Omega: \phi(x,y) < 0\} \end{cases}$$

3.4. Gaussian mixture model (GMM)

Another segmentation method is connected with Gaussian mixture model. In this method, it is necessary to create a mask which specify foreground and background of the picture. This mask covers the image and then based on this input. Further the probability is calculated to get a distribution based on GMM from the pixels under the mask. K-means [7] algorithm is used for clustering.

$$\sum_{k=1}^{K} \phi_k \mathcal{N}(x; \mu_k, \Sigma_k) = \sum_{k=1}^{K} \frac{\phi_k}{\sqrt{(2\pi)^D |\Sigma_k|}} e^{-\frac{1}{2}(x-\mu_k)^T \Sigma_k^{-1}(x-\mu_k)} \quad (4)$$

$$p_y(x_t) = p(x_t, \theta_y) = \sum_{k=1}^{K} \phi_{y,k} \mathcal{N}(x_t; \mu_{y,k}, \Sigma_{y,k}) \quad (5)$$

where ϕ_k is prior probability, μ_k is mean vector, Σ_k is covariance matrix, $\mathcal{N}(x; \mu_k, \Sigma_k)$ is multivariate normal distribution.

4 Results

4.1. Pre-processing (+entropy)

The graph below (Fig. 5.) shows the entropy value of original image and its variations. The green channels have the lowest value so it means that segmentation in this channel should give the best results, in case of the low level of the natural noise.

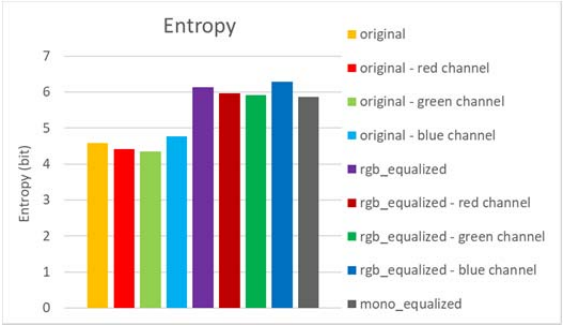

Fig. 5. Entropy of the original image and its variations.

On Fig. 7 is shown the histogram of the pixels under the mask from the original image (Fig. 6.) and on Fig. 9. is histogram of the equalized image (Fig. 8.).

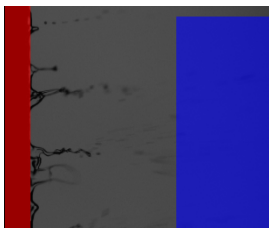

Fig. 6. Original image with mask.

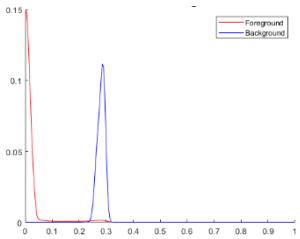

Fig. 7. Histogram of the masked pixels from the original image.

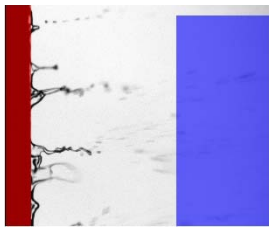

Fig. 8. Equalized image.

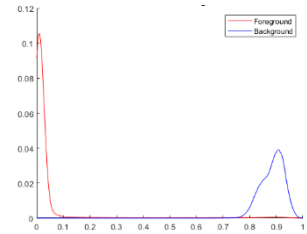

Fig. 9. Enhanced histogram.

4.2. Thresholding (TH)

In segmentation using thresholding is well visible difference between the RGB channels of the image. On Fig. 10. One can see noise on the right side of the image in compare with Fig. 11. And result from red channel gives the lowest number of segmented pixels.

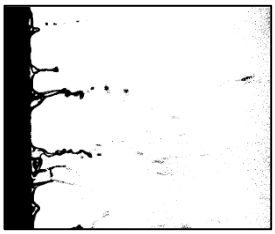

Fig. 10. Segmented blue channel of original image using thresholding (threshold = 0,74).

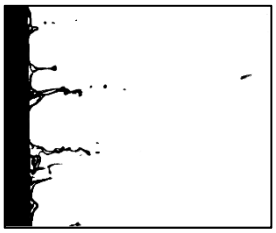

Fig. 11. Segmented green channel of original image using thresholding (threshold = 0,74).

On the graph below (Fig. 12.) one can see liquid content ratio (LCR) for images segmented by thresholding and GMM.

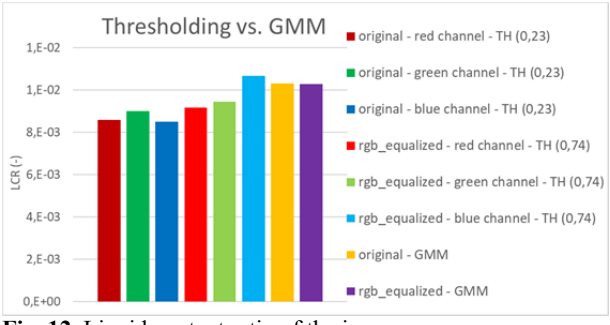

Fig. 12. Liquid content ratio of the images.

4.3. Active contour (AC)

The Fig. 13. and Fig. 14. show segmented images using active contour. One can see that it differs from

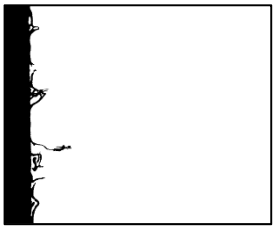

Fig. 13. An original image segmented using active contour.

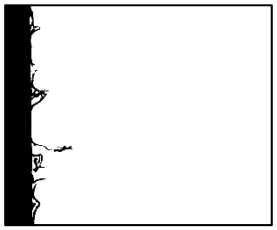

Fig. 14. An equalized image segmented using active contour.

segmented image using thresholding and using GMM. On the graph below (Fig. 15.) one can see liquid content ratio (LCR) for images segmented by active contour and GMM. The LCR value does not differ within AC segmentation, so it means that enhancement of the image does not impact the final segmentation, nor within GMM segmentation.

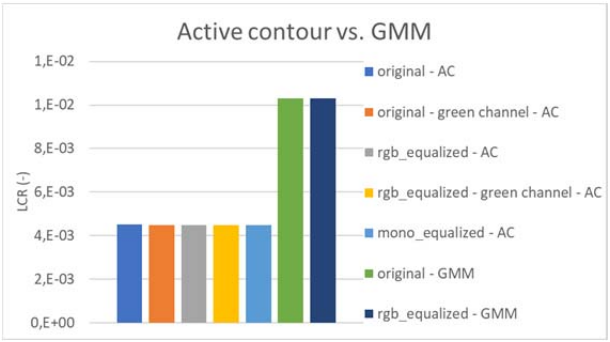

Fig. 15. Liquid content ratio of the images.

Different number of iteration was tested, started at 100 ended at 1500. After 500 iteration the results stopped varying.

4.4. Gaussian mixture model (GMM)

Segmentation using GMM gave the same results for original image and for enhanced image, even for different number of iterations. This method seems to be the most stable.

Sample RGB values and estimated GMMs. are shown on Fig. 16. The Fig. 17. and Fig. 18. show the segmented images.

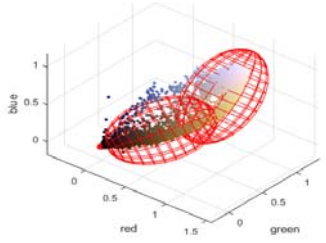

Fig. 16. Sample RGB values and estimated GMMs.

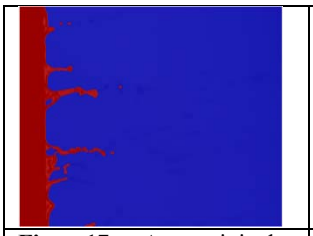

Fig. 17. An original image segmented using GMM.

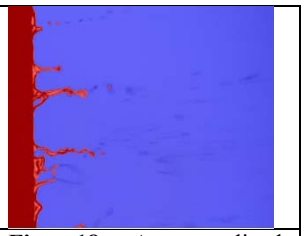

Fig. 18. An equalized image segmented using GMM.

5 Conclusion

In this contribution are presented several image processing methods used for the description of the liquid films disruption. The knowledge of the liquid disruption in the steam turbines is described mostly phenomenologically [8] and for the future development would be useful to have some tool for quantitative analysis. The entire image capturing process is difficult due to the high velocity of the flowing air over the airfoil. The exposure time is very short and this reasons limiting the quality of the mages. The suggested image processing methods are suitable for the analysis of the images of the liquid atomization but seem to be necessary to find another combination of the methods parameters. One possibility is application of the nonlinear equalization.

We gratefully acknowledge the support by the Grant Agency of the Czech Technical University in Prague, Grant No. SGS 13/18 and National Centre for Energy TN01000007.

References

1. O. Bartoš, X. Cai, M. Kolovratník, EPJ Web of Conferences. 2014, vol. 67, ISSN 2100-014X
2. O. Bartoš, X. Cai, M. Kolovratník, *Experimental investigation of coarse water droplets in steam turbines by the adapted photogrammetry method*. In The Baumann Centenary Conference … Cambridge: ISBN 978-0-903428-35-4
3. M.Hoznedl, at al.. Experimental research on the flow at the last stage of a 1090 MW steam turbine. *Proceedings of the Institution of Mechanical Engineers, Part A: Journal of Power and Energy*. 2018, DOI: 10.1177/0957650917749692.
4. M. Kolovratník, at al: *Nanoparticles found in superheated steam – A quantitative analysis of possible heterogeneous condensation nuclei.* Proceedings of the Institution of Mechanical Engineers Part A - Journal of Power and Energy. 2014, vol. 228, no. 2, p. 186-193. ISSN 0957-6509
5. C.F. Bohren, D.R. Huffman *Absorption and Scattering of Light by Small Particles*. John Wiley & Sons, Inc., USA (1998)
6. Z. Fu, L. Wang, *Color Image Segmentation Using Gaussian Mixture Model and EM Algorithm*. In: Wang F.L., Lei J., Lau R.W.H., Zhang J. (eds) Multimedia and Signal Processing. CMSP 2012. Communications in Computer and Information

Science, vol 346. Springer, Berlin, Heidelberg, ISBN 978-3-642-35285-0
7. T. F. Chan, L. A. Vese, *Active contours without edges*. IEEE Transactions on Image Processing, Volume 10, Issue 2, pp. 266-277, 2001
8. H. Liu, *Science and engineering of droplets: fundamentals and applications*. Norwich, NY: Noyes Publications, c2000. ISBN 0-8155-1436-0